

Rapid Probabilistic Interest Learning from Domain-Specific Pairwise Image Comparisons

Michael Burke, Siyabonga Mbonambi, Purity Molala, Raesetje Sefala

Mobile Intelligent Autonomous Systems

Council for Scientific and Industrial Research

Pretoria, South Africa

Contact author: michaelburke@ieee.org

Abstract—A great deal of work aims to discover large general purpose models of image interest or memorability for visual search and information retrieval. This paper argues that image interest is often domain and user specific, and that efficient mechanisms for learning about this domain-specific image interest as quickly as possible, while limiting the amount of data-labelling required, are often more useful to end-users. This work uses pairwise image comparisons to reduce the labelling burden on these users, and introduces an image interest estimation approach that performs similarly to recent data hungry deep learning approaches trained using pairwise ranking losses. Here, we use a Gaussian process model to interpolate image interest inferred using a Bayesian ranking approach over image features extracted using a pre-trained convolutional neural network. Results show that fitting a Gaussian process in high-dimensional image feature space is not only computationally feasible, but also effective across a broad range of domains. The proposed probabilistic interest estimation approach produces image interests paired with uncertainties that can be used to identify images for which additional labelling is required and measure inference convergence, allowing for sample efficient active model training. Importantly, the probabilistic formulation allows for effective visual search and information retrieval when limited labelling data is available.

I. INTRODUCTION

Video cameras are increasingly deployed in exploration, monitoring and surveillance applications. These cameras produce vast amounts of information, which needs to be condensed into manageable quantities for both storage and human evaluation. While compression can address the former, this does not aid users, who are often faced with the daunting task of analysing lengthy video sequences or large collections of images. Systems that automatically flag interesting images or information and present a summary to an operator are required to remedy this. This is particularly important in visual search and retrieval applications, where end-users desire highly relevant content, with minimal noise. The ability to predict user preferences reliably is crucial to realising this.

Unfortunately, it can be hard to define the concept of interesting content, as this is typically context dependent. For example, [12], which investigates the feasibility of classifying images by scientific value to address bandwidth constraints on a Mars rover, shows that domain experts from different

Authors listed alphabetically, this work was completed during an internship at the CSIR, as part of the CSIR D-SIDE programme. M Burke was supported by funding from CSIR young researcher's establishment grant, YREF032.



Fig. 1. A pairwise comparison website is used to source image comparisons suitable for use in a Bayesian ranking system. For the coastal dataset shown here, the right image is preferable, because regions of wet and dry sand are more easily distinguishable than those in the left image.

fields value and rank images differently. As a result, numerous approaches have attempted to build models that can identify content of interest to end-users. These often rely on ranking systems leveraging pairwise comparisons obtained as part of a training phase, but this process can be expensive and time-consuming.

More recently, a great deal of work has aimed to develop general models of image interest relying on large general-purpose training databases, in an attempt to avoid retraining models for multiple applications and the need to repeatedly crowd-source training data. However, in this work we argue that domain specific models are still extremely important to end-users. Here, the ability to rapidly train a model suitable for end-user applications with minimal data labelling required is highly desirable. This work introduces a rapid learning approach for domain specific image interest prediction using pairwise image comparisons. Here, pairwise image interest comparisons (Figure 1) are used to infer image interests using a probabilistic ranking algorithm, and a Gaussian process smoother is then used to improve these estimates by taking into account image similarities using features extracted by a pre-trained convolutional neural network.

This approach can speed up the learning process significantly, requiring far fewer image comparisons to be labelled to outperform probabilistic benchmark algorithms. In addition, domain-specific models of image interest can be used to produce user-driven storyboards.

The proposed approach targets small-data problems that

regularly confront end-users working in specific domains. Here, end-users often need to identify content of interest in small unlabelled datasets, often comprising no more than a few thousand images. These images are often captured at great expense, and the requirements of domain experts and labelling complexity can limit solutions. In this case, pairwise comparison labelling provides a simple, turnkey mechanism of identifying end-user needs, and the design of a problem specific labelling interface is not required.

The primary contributions of this work are as follows:

- A fully probabilistic image interest estimation scheme is introduced, allowing for image retrieval and ranking with a measure of uncertainty.
- We show how this measure can be used to determine when sufficient data labelling has been obtained, allowing for sample efficient model training.
- We show that Gaussian process smoothing in high dimensional image feature space is more effective at image ranking than state of the art neural models when labelling data is limited.

II. RELATED WORK

As mentioned earlier, the concept of image interest can be rather subjective. This difficulty in defining image interest has led to a wide range of work being conducted in multiple areas seeking to address this topic. We briefly discuss these below, with reference to related work in novelty detection, video storyboarding, image interest and image memorability.

A common definition of interest relates to novelty, with interest determined by the frequency of occurrence of an event or observation. Novelty detection is often framed as an outlier detection problem. For example, dynamic time warping has been used to align image feature sequences for a life-logging application, with the alignment quality determining novelty [3]. Here, the authors leverage the fact that people typically experience day-to-day repetition, and assume that areas of mismatch or disagreement with typical daily activity should be flagged as novel. If prior information about the environments or observations to be encountered is available, domain-based approaches to novelty detection are particularly effective. Here, classifiers are trained to recognise expected samples, with any misclassification flagged as novel. For example person, car and groups of person classifiers are trained for a surveillance application by Dieh et al. [16], with classification failures listed as novel. Terrain classification using support vector machines is applied by Brooks and Iagnemma [9], with negative training data in the form of unlabelled images used to model novelty.

In contrast to novelty-based image recognition, storyboarding aims to summarise lengthy video sequences using a reduced set of images likely to interest an end-user. This is particularly useful for search and retrieval applications, where users are unwilling to watch a full video in order to evaluate its content. An overview of video storyboarding approaches is provided by Bolaños et al. [8].

Most storyboarding approaches operate by first segmenting sequences into shots or sub-sequences, and then selecting a representative image for each shot. For example, Ngo et al. [39] use a graph-based clustering approach to segment video into static, panoramic, zoom, motion and in-deterministic shots. An attention model trained on a number of low level features is then used to rank the frames in each shot. This approach provided good performance when the informativeness and enjoyability of the keyframes it produced were evaluated by users. Shots are also used by Srinivasan et al. [46], with these segmented by detecting changes in image colour histograms. The authors note that scrolling through images is still tedious, so aggregate keyframes selected from shots to form a new video summary of the type typically available for preview in online video repositories.

MPEG-7 image features have been used in conjunction with image intensity histograms to rank the relevance of images relative to other frames [56]. Video sequence transitions are detected in [34] by tracking image changes, and selecting keyframes most similar to the average of all frames in shots. Shots selected by detecting video frame transition effects may not be well described using a single key-frame, and a statistical run test is used by Mohanta et al. [37] to segment shots into sub-shots before key-frame selection.

Objects are tracked in image sequences by Guleryuz and Ratnakar [19], with images ranked by the length of time objects remain present. A representative frame is selected by finding the frame in each tracked sub-sequence for which the largest number of tracked pixels are present. A people-centric storyboarding approach is taken by Vonikakis et al. [52], with crowd-sourcing used to identify user preferences when composing slide shows, focusing on facial features and image quality.

Video storyboarding is of particular interest in life-logging applications, where large amounts of data need to be summarised. Here, egocentric cameras are used to record the daily activities of their wearers. Image sequences of this type often have low temporal consistency, as images are not saved constantly due to storage constraints, so change-based shot segmentation approaches tend to fail. An attempt to remedy this is made by Bolanos et al. [6], who use an energy minimisation segmentation approach on low level image features to classify images as static, moving camera or in transit. In later work, Bolaños et al. [7] use a pre-trained convolutional neural network to identify image features for use in event segmentation for egocentric photo streams.

The storyboarding approaches discussed thus far do not necessarily produce keyframes that are likely to be of interest to humans. In an attempt to remedy this, personalised video summaries are produced by Varini et al. [51] by incorporating a prior on the type of information of interest. Here, a natural language request for images is used to retrieve images in a similar category. Gaze fixation clustering was used by Damen et al. [14] to discover areas that are likely to be interesting to humans. Instead of detecting keyframes using novelty, high quality images are found by Xiong and Grauman [58]. Here, a

generative model of ‘snaps’ is trained using an online database of images, under the assumption that most images in online databases are photographs intentionally taken by users and have good composition. Storyboards are formed by segmenting events temporally and selecting keyframes that agree most with this ‘snap’ prior. This approach is particularly effective and has been used for an exploring mobile robot [58].

The subjective and contextual nature of image interest makes it hard to design a bottom up interest detection algorithm. Instead, a far more sensible approach makes use of operator supervision to learn about interest. Relative image comparisons are an intuitive way to infer user preference [20], and frequently used for image ranking because they can provide more stable and useful rankings than individual image-based scoring systems [27].

Pairwise ranking systems are particularly popular across a broad range of problems, and have been used for optimising visual search [32], noise reduction in support of highlight detection in video [28] and visual re-ranking in information retrieval [49]. The latter proposes a Bayesian visual re-ranking approach, which re-orders search results using a posterior distribution combining noisy image search results obtained using text queries (a likelihood measure) and an image similarity prior based on block-wise colour moments. Our approach is similar to this, in that we introduce an image similarity prior using a Gaussian process fit over image features extracted using a convolutional neural network, but we combine this with a likelihood inferred from pairwise image comparisons labels returned from end-users instead of queried textual search results. In addition, the use of the Gaussian process prior limits the number of parameters required, as the majority of these are inferred during model training.

Pairwise ranking is also often used to estimate multimedia quality or predict user preferences. For example, [33] use pairwise ranking to infer image quality from subjective quality score labels, while [47] apply pairwise comparisons to recommend appropriate image filters in social media applications. Here, Amazon Mechanical Turk crowd-sourcing was used to solicit filter preferences from users presented with image pairs in various categories. A convolutional neural network trained to identify image categories was then used to propose suitable image filters, based on the inferred preferences.

A number of effective ranking algorithms have been developed for ranking using pairwise comparisons. Ranking systems such as the Elo chess rating system [18] and TrueSkill [23], a Bayesian ranking scheme extension to Elo, account for relative player skills and performance inconsistency.

TrueSkill is applied ubiquitously in image ranking systems, providing an effective approach to estimating image interest for a wide range of applications. For example, Hipster wars [27] uses TrueSkill to train an image-based style classifier in a fashion application from style judgements, using a part-based model to generate saliency maps that associate clothing items with styles, CollaboRank [24] uses pairwise comparisons to rank images according to a number of case-based queries (positiveness, perceived threat level, celebrity or film

popularity), the Matchin approach [20] uses a two player pairwise comparison game to extract a global image ‘beauty’ rank and Streetscore [38] predicts the perceived safety of street scenes using binary answers to the question “Which place looks safer?”. Here, TrueSkill was used to infer street scene safety measures using over 200 000 pairwise image comparisons obtained for approximately 4 000 images. A support vector machine (SVM) was then trained to predict these safety measures using a variety of image features, and then used to build perception maps of city safety in the United States. Unfortunately, this decoupling of SVM interest prediction from the ground truth image interest inference process using TrueSkill means that a highly intensive labelling process is required, with approximately 16 comparisons per image needed to provide interest estimates with high enough levels of certainty for SVM training [38]. This paper shows how this process can be coupled by combining TrueSkill with a Gaussian Process smoother in image feature space, thereby speeding up the labelling process. This coupling is probabilistic and takes interest uncertainty into account so fewer image comparisons are required.

In contrast to approaches that attempt to infer interest scores from pairwise comparisons, a number of techniques learn to rank directly using these comparisons. These approaches are typically formulated as optimisation problems. For example, Ma et al. [33] learn a linear image feature projection that minimises a binary comparison objective based on image quality, while ranking SVMs [25] learn a projection by maximising a Kendall τ objective (a measure based on the number of concordant and discordant ranked pairs in a list). More recently, this pairwise loss function has been used to train ranking neural networks directly [17, 53], allowing for algorithms that scale to larger datasets, while incorporating the advantages of deep learning. Dubey et al. [17] extend Streetscore to consider additional street scene attributes, and capture a significantly larger dataset for experimentation. In order to deal with the challenges of this large dataset, they train a multi-layer neural network to rank image pairs using the ranking SVM loss in combination with an attribute classification loss, and using image features extracted by a pre-trained convolutional neural network. As noted by the authors, coupling the ranking process with image features improves upon traditional two-step processes [17]. However, this approach is not necessarily concerned with the data labelling process, and still assumes that a large representative set of comparisons is already available. In addition, this ranking loss does not account for images that are perceptually similar, for which comparison outcomes may differ when repeated. The probabilistic ranking process described in this paper addresses these challenges.

Pairwise comparisons have also been used to rank abstract paintings according to the emotional responses they elicit [43], to evaluate the representativeness of images extracted from twitter timelines [55], and to determine appropriate facial expressions for portraits using images extracted from short video sequences [60]. Unfortunately, the crowd-sourcing

process used to obtain pairwise comparison results can be time consuming and expensive [1] and a large number of comparisons are typically required to infer interests. In an attempt to remedy this, heuristic budget constraints are introduced into a pairwise ranking process by Cai et al. [11], while Burke [10] proposes a smoothing algorithm that uses the temporal image interest similarity present in video to improve interest estimates with fewer comparisons. The latter relies on a Markovian assumption, and so fails to account for interest similarity that is likely to occur when images are captured in the same place at different times, or if images themselves appear similar. This paper introduces a Gaussian process smoother that addresses this limitation.

More recently, there have been attempts to train more general models of image interest, most notably for the 2016 [44] and 2017 Predicting Media Interestingness MediaEval challenges [15]. For the 2017 task, interestingness is defined within the context of extracting frames and film excerpts that would aid a user to make a decision about whether they would be interested in watching a movie. This task is relatively general purpose, as movies cover different topics and genres, but inevitably favours aesthetics and genre or emotional content in the definition of interest. As a result, prediction methods that introduce genre prediction systems and related contextual information tend to perform well on this task. For example, Ben-Ahmed et al. [4] use a deep neural network to predict genres from image interests, and a SVM to predict genres from audio features. The genre logits obtained from these models are then used as a multimedia representation, and a final SVM is trained using these to predict a binary image interest value. Berson et al. [5] use a broad range of information (image features, image captioning representations, audio features, and representations extracted from textual meta-data) within a large multimodal neural network framework to predict a binary image interest value, noting that the inclusion of contextual information like image captions and textual meta-data can lead to over-fitting on individual image interest prediction tasks, but improved performance on video interest prediction.

The Predicting Media Interestingness challenge was adapted to become a memorability prediction challenge in 2018 [2]. Memorability is closely related to image interest, and typically measured using an experimental approach where users are shown a sequence of images, with some repeated, and asked to recall which images they have seen previously. Khosla et al. [26] carried out a comprehensive study of memorability and made an extremely large database of memorability scores and associated images available. Here, image memorability was shown to relate to image popularity and emotional content, but not necessarily to aesthetics.

While an effective measure of image interest, memorability may be unsuited for domain-specific small to medium scale computer vision problems, as the labelling burden on end-users can be excessive. This work seeks to highlight the subjective nature of image interest through a number of domain-specific cases and to emphasise that for many use cases, domain-specific models of interest are needed. This typically requires

an intensive labelling process, but this work shows that a Gaussian process smoother combined with a Bayesian ranking system can infer image interest scores in a stable and efficient manner, providing information about interest prediction certainty, thereby facilitating more rapid deployment of models.

III. IMAGE INTEREST ESTIMATION

Our goal is to use pairwise image comparisons to train a model that can predict image interest. This model can then be used for image storyboarding. Initially, a baseline Bayesian ranking scheme is used to estimate image interest scores. This is combined with a Gaussian process smoother that improves estimates by incorporating image similarity information from convolutional neural network image features. We compare this probabilistic approach with a deep learning approach using a pairwise loss function.

A. Probabilistic image ranking

This work uses the TrueSkill Bayesian ranking scheme [23] to compute image interest scores. TrueSkill is a probabilistic ranking system that assumes players in a game have respective skills, w_1 and w_2 , and that game outcomes can be predicted by the performance difference between skills, subject to Gaussian noise effects.

For image pairs,

$$t \sim \mathcal{N}(s, 1) \quad (1)$$

models the interest difference between two images, with $s = w_1 - w_2$ the interest difference and the standard normal distribution accounting for potential labelling errors [10]. Comparison outcomes are given by $y = \text{sign}(t)$, with a positive y indicating a win for image 1, and a negative y indicating a loss.

Interest estimation under this model can be treated as a Bayesian inference problem, with the posterior over skills described by

$$p(w_1, w_2 | y) = \frac{p(w_1)p(w_2)p(y|w_1, w_2)}{\int \int p(w_1)p(w_2)p(y|w_1, w_2)dw_1dw_2}, \quad (2)$$

where $p(w_i) = \mathcal{N}(\mu_i, \sigma_i^2)$ is a Gaussian prior over image interests and

$$p(y|w_1, w_2) = \int \int p(y|t)p(t|s)p(s|w_1, w_2)dsdt \quad (3)$$

the likelihood of a game outcome given interests. The model above is easily extended to multiple images, \mathbf{w} , by chaining comparisons, \mathbf{y} , together in a large graph, producing the posterior $p(\mathbf{w}|\mathbf{y})$. This posterior is intractable, but can be estimated numerically and approximated by a Gaussian [36]

$$p(\mathbf{w}|\mathbf{y}) \sim \mathcal{N}(\mathbf{w}_m, \Sigma_n), \quad (4)$$

with mean \mathbf{w}_m and variance Σ_n .

B. Temporal TrueSkill

The interests inferred using TrueSkill are only updated for those images involved in pairwise comparisons. As a result, a large number of comparisons could be required to infer interest values to an acceptable level of certainty when image datasets are large. However, where image interests are required for image sequences or video datasets, a simple posterior smoothing process [10], hereafter referred to as temporal TrueSkill (TTS), can be used to improve the TrueSkill estimates.

Here, image interests in a video sequence are assumed to follow a random walk motion model $p(x_k|x_{k-1})$, and image distributions inferred using TrueSkill used as measurement models for the k -th image in a sequence of K images, $p(w_k|x_k)$, within a standard Rauch-Tun-Striebel smoother [41], to provide a posterior distribution over image interests, conditioned on a sequence of TrueSkill estimates, $p(x_k|w_{1:K})$,

$$\begin{aligned} p(x_k|w_{1:k-1}) &= \int p(x_k|x_{k-1})p(x_{k-1}|w_{1:k-1})dx_{k-1} \\ p(x_k|w_{1:k}) &= \frac{p(w_k|x_k)p(x_{k-1}|w_{1:k-1})}{p(w_k|w_{k-1})} \\ p(x_k|w_{1:K}) &= \int \frac{p(x_{k+1}|x_k)p(x_k|w_{1:k})}{p(x_{k+1}|w_{1:k})} \times \\ &\quad p(x_{k+1}|w_{1:K})dx_{k+1}. \end{aligned} \quad (5)$$

Temporal TrueSkill is computationally inexpensive, but fails to account for similarities with images themselves. The Gaussian process (GP) interest refinement proposed here addresses this limitation.

C. Gaussian process interest refinement

As an alternative to the smoothing algorithm used for TTS, this work refines image interest estimates obtained using TrueSkill using a Gaussian process smoother operating in image feature space. A GP is a collection of random variables, where any finite number have a joint Gaussian distribution [40]. Gaussian processes,

$$f(\mathbf{x}) \sim \mathcal{GP}(m(\mathbf{x}), k(\mathbf{x}, \mathbf{x}')), \quad (6)$$

are specified by the mean function $m(\mathbf{x})$ and the covariance function $k(\mathbf{x}, \mathbf{x}')$ of a real process $f(\mathbf{x})$,

$$m(\mathbf{x}) = \mathbb{E}[f(\mathbf{x})] \quad (7)$$

$$k(\mathbf{x}, \mathbf{x}') = \mathbb{E}[(f(\mathbf{x}) - m(\mathbf{x}))(f(\mathbf{x}') - m(\mathbf{x}'))]. \quad (8)$$

For the image interest application, the domain \mathbf{x} is over a set of image attributes or features associated with an image, while f is the process that gives rise to image interest. \mathbf{x}' denotes the features or attributes associated with captured image interest random variables $\mathbf{w} = [w_1 \dots w_N]$, where N denotes the number of images. The mean function $m(\mathbf{x})$ is assumed to be zero in this work.

Under this process, a likelihood for image interests, \mathbf{w} , can be formed,

$$p(\mathbf{w}|\mathbf{x}, f) \sim \mathcal{N}(f(\mathbf{x}), \Sigma(\mathbf{x})). \quad (9)$$

Using this likelihood in conjunction with a GP prior,

$$p(f) \sim \mathcal{GP}(\mathbf{0}, k(\mathbf{x}, \mathbf{x}')), \quad (10)$$

and taking advantage of the marginalisation properties of Gaussian processes, leads to a Gaussian process posterior [40],

$$p(f|\mathbf{x}, \mathbf{w}) \sim \mathcal{GP}(m_p, k_p), \quad (11)$$

where

$$m_p = \mathbf{T}(\mathbf{X}, \mathbf{X}')\mathbf{w}_m, \quad (12)$$

$$k_p = K(\mathbf{X}, \mathbf{X}') - \mathbf{T}(\mathbf{X}, \mathbf{X}')K(\mathbf{X}, \mathbf{X}'), \quad (13)$$

and

$$\mathbf{T}(\mathbf{X}, \mathbf{X}') = K(\mathbf{X}, \mathbf{X}')[K(\mathbf{X}', \mathbf{X}') + \Sigma(\mathbf{X}')]^{-1}. \quad (14)$$

Assuming N training images with features \mathbf{X} , and N' query images with features \mathbf{X}' , $K(\mathbf{X}, \mathbf{X}')$ denotes the covariance matrix formed by evaluating $k(\mathbf{x}, \mathbf{x}')$ for all pairs of training and test features. $\Sigma(\mathbf{X}') = \Sigma_n$ is a diagonal matrix with diagonals corresponding to the variance in estimated image interests \mathbf{w}_m , obtained from the TrueSkill posterior in (4). Equation (11) can be used for interest prediction by evaluating the GP posterior for a set of images with features \mathbf{X}^* ,

$$p(\mathbf{w}^*|\mathbf{X}^*, \mathbf{X}', \mathbf{w}) \sim \quad (15)$$

$$\mathcal{N}(\mathbf{T}(\mathbf{X}^*, \mathbf{X}')\mathbf{w}_m, K(\mathbf{X}^*, \mathbf{X}')\mathbf{T}(\mathbf{X}^*, \mathbf{X}')K(\mathbf{X}^*, \mathbf{X}')).$$

A wide variety of covariance functions can be used, but for this work we apply a radial basis function kernel to ensure smooth interests over image feature space,

$$k(\mathbf{x}, \mathbf{x}') = \exp\left(-\frac{D(\mathbf{x}, \mathbf{x}')}{2l^2}\right). \quad (16)$$

Here, l is a length scale hyperparameter used to control the level of similarity at which image attributes affect one another, and D is a distance measure appropriate to the image attributes selected for smoothing. The image attributes considered here comprise d -dimensional image features extracted using a pre-trained convolutional neural network [48], while the cosine distance,

$$D(\mathbf{x}, \mathbf{x}') = 1 - \frac{\mathbf{x} \cdot \mathbf{x}'}{\|\mathbf{x}\|\|\mathbf{x}'\|}, \quad (17)$$

is used as the distance measure. Figure 2 illustrates the image interest inference and smoothing approach described above, referred to as GP-TS hereafter.

Gaussian processes are memory intensive, $\mathcal{O}(N^3)$, so are often considered unsuitable for large image datasets. However, given that our goal is to learn about image interest for the small-data regime where limited numbers of images and labels are required, this is typically not problematic. For larger datasets, sparse Gaussian processes [22] or Bayesian committee machines [50] reduce this complexity significantly.

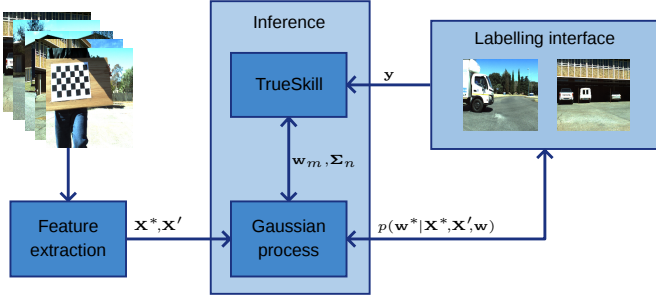


Fig. 2. The GP-TS image interest prediction process is depicted above. Input images are fed into a deep convolutional neural network, producing a d -dimensional feature vector. This feature vector is then fed into a Gaussian process that is trained using image features and corresponding TrueSkill image interest estimates, inferred using pairwise comparison labels.

D. GP-TS Inference

We consider a number of approaches to perform probabilistic inference under the GP-TS model. The first decouples inference using the Gaussian process and Trueskill, with inference performed separately for each component. Here, inferred image interest levels are initially estimated using expectation propagation [36] under the Trueskill model. Expectation propagation approximates factors in the model using Gaussian distributions fit through moment matching, which allows for efficient inference by message passing. This produces the approximate posterior in (4), with mean interest estimates and uncertainties for each image in the set conditioned on image comparison outcomes. This distribution over image interests can then be used to perform inference under a Heteroscedastic Gaussian process model [31], with the length scale parameter l inferred using maximum a-posteriori estimation.

As an alternative, inference under the GP-TS model can be treated in a fully Bayesian manner with appropriate priors over parameters. In this case, we construct the GP-TS generative model as follows, with parameter definitions unchanged from previous sections:

$$\begin{aligned}
 l &\sim \text{Half Cauchy}(\beta = 0.5) \\
 \Sigma_n &\sim \text{Half Cauchy}(\beta = 1) \\
 \mathbf{f}(\mathbf{x}) &\sim \mathcal{GP}(\mathbf{0}, k(\mathbf{x}, \mathbf{x}')) \\
 \mathbf{w}^* &\sim \mathcal{N}(\mathbf{f}, \Sigma_n) \\
 p &= \text{Sigmoid}(w_i^* - w_j^*) \\
 y &\sim \text{Bernoulli}(p).
 \end{aligned} \tag{18}$$

Here, length scale l and interest uncertainty Σ_n are modelled using half Cauchy priors. The zero-mean Gaussian process prior over features extracted from images using a pre-trained convolutional neural network is used to model image interest. The marginal likelihood of this prior, which incorporates labelling inconsistency noise, provides a predictive distribution for image interests given image features. Comparison outcomes are modelled as a Bernoulli trial given a probability formed by passing the difference in interests (w_i^*) and (w_j^*), between the image pairs through a sigmoid function. This model allows for variational Bayesian inference strategies

such as automatic differentiation variational inference [30] to be applied. Like expectation propagation, variational inference approximates distributions using a family of simpler distributions, framing inference as a task of minimising the Kullback-Liebler divergence of samples from the posterior (training data) from the simpler target distributions. This approach allows for efficient parallel batch estimation, leveraging many advances in gradient-based optimisation for deep learning. In this work, we use the PyMC3 probabilistic programming library [42] for inference.

Inference in the fully Bayesian setting can be expensive, so we also consider the use of Gaussian process approximations such as sparse Gaussian processes [22], which rely on factorisation to reduce the computational complexity of GP's to $\mathcal{O}(NM^2)$. Here, M is a parameter controlling the number of input features to use for estimating the Gaussian process kernel.

E. Pairwise loss ranking

A deep learning approach, trained directly using pairwise comparisons to minimise a pairwise loss function [17, 53] can be used as an alternative to the probabilistic approaches described above. Here, image features are first extracted from each image in a comparison pair using a pre-trained convolutional neural network. These features are then fed into two weight-tied multi-layer fully connected neural networks (typically 2-3 layers using ReLU activation functions) producing scalar outputs y and x , and trained to minimise the loss,

$$\text{PWL} = \sum_{i=1}^n \text{ReLU}(y - x), \tag{19}$$

using stochastic batch gradient descent. This loss is equivalent to a ranking SVM loss [25], but has been simplified here by assuming that the comparison winner is always input to the network producing y . This approach is referred to as FC-PWL hereafter.

IV. STORYBOARDING

The image interest estimates obtained using pairwise ranking systems are easily used for storyboarding. This is a simple matter of selecting N_s images corresponding to the top mean image scores, requiring that these are at least d_s images apart for sequential datasets. Here, both d_s and N_s are left as user defined input parameters, to allow for customised and controllable storyboarding. Giving a user the ability to adjusting these parameters and display relevant results within an exploration tool is a particularly effective means of exploring image datasets.

A similar approach can be taken to produce image memorability-based storyboards. In this work, we compare GP-TS storyboards with those produced using a pre-trained image memorability predictor, MemNet [26]. MemNet is a deep convolutional neural network trained using 60 000 images sampled from a number of image collections (both scene and object-centric) and corresponding memorability scores, captured using an intensive labelling process.

As an alternative to storyboarding using image interest or memorability, clustering approaches to storyboarding attempt to summarise image datasets by finding a representative set of images. In this work, we also compare GP-TS and MemNet storyboarding with a recent clustering approach [7]. Here, hierarchical agglomerative clustering [54] is applied to the same pre-trained convolutional neural network image features used by GP-TS. After grouping images into N_s clusters, a representative image is selected for each cluster by finding the image with a feature vector closest to the mean image feature vector for each cluster. This clustering approach to storyboarding is termed HAC hereafter.

V. DATASETS

The proposed approach to turnkey image interest estimation and storyboarding was investigated using five distinct datasets. Each of these is briefly described below.

A. OASIS

The first dataset used for testing is a small publically available medical imaging dataset of 416 averaged and co-registered T1-weighted cross-sectional magnetic resonance imaging scans of patients with varying levels of dementia [35]. The scans are normalised and accompanied by meta-data that includes normalised brain volume measurements. Pairwise comparison results were simulated by generating 15 000 comparison outcomes using the normalised brain volume measurements. Here, we assume that brain volume reductions correlate with those images of patients depicting reduced brain matter, and that a domain expert would consider images with reduced brain matter of importance. The 15 000 comparison results, $\mathbf{G}_{\text{baseline}}$, were split into test, \mathbf{G}_{test} , and training, $\mathbf{G}_{\text{train}}$, sets, comprising 5 000 and 10 000 comparisons respectively.

B. Violence

The second dataset used for testing is a publically available dataset of over 10 000 protest images [57], with accompanying measures of the perceived violence depicted therein. As before, pairwise comparison results were simulated by generating 15 000 comparison outcomes using these perceived violence scores. Here, it was assumed that an end-user would be interested in identifying scenes depicting violence. Unlike the dataset above, the perceived violence dataset is already divided into test (2 342 images) and training (9 316 images) sets. In order to align with this division, we split the 15 000 comparison results obtained from the training set, $\mathbf{G}_{\text{baseline}}$, into 5 000 test examples, \mathbf{G}_{test} , and 10 000 training examples, $\mathbf{G}_{\text{train}}$, but also generated an additional test set, $\mathbf{G}_{\text{test}}^2$, of 10 000 comparisons using images sampled at random from the perceived violence test images, $\mathbf{G}_{\text{baseline_test}}$. Results are reported for both of these test sets.

C. CSIR

The third dataset comprises 4 000 outdoor images captured by an autonomous rover containing a sequence of images captured in an uncontrolled outdoor environment. Here, 15

000 baseline pairwise image comparison results, $\mathbf{G}_{\text{baseline}}$, were obtained using a labeling interface (Figure 1) that presented randomly selected pairs of images to a single robot operator and asked which image was more useful to them. In general, the robot operator (wary of potential collisions) favoured images that contained cars or pedestrians. As before, the 15 000 baseline image comparisons were split into test, \mathbf{G}_{test} , and training, $\mathbf{G}_{\text{train}}$, sets, comprising 5 000 and 10 000 comparisons respectively.

D. Coastcam

The fourth dataset consists of almost 2 000 outdoor images of the Fishhoek coastline in South Africa, captured from a static camera [10]. Here, 10 000 baseline pairwise image comparison results, $\mathbf{G}_{\text{baseline}}$, were obtained by presenting randomly selected pairs of images to a single domain expert and asking which image was more important (Figure 1). The domain expert favoured images that showed images where wet and dry sand regions were clearly identifiable. As before, the baseline image comparisons were split into test, \mathbf{G}_{test} , and training, $\mathbf{G}_{\text{train}}$, sets, comprising 3 300 and 6 700 comparisons respectively.

E. Place Pulse 2.0

The final dataset used for testing comprises 110 988 Google Streetview images taken from 56 cities [17]. Here, over 1 million baseline pairwise image comparisons were captured and made publically available for six perceptual attributes: safe, lively, boring, wealthy, depressing and beautiful. In this work, only the safety attribute is considered, with 323 392 comparisons. These baseline image comparisons $\mathbf{G}_{\text{baseline}}$ were split into test, \mathbf{G}_{test} , and training, $\mathbf{G}_{\text{train}}$, sets, comprising 106 720 and 216 672 comparisons respectively. This dataset is used to test the scalability of the proposed approach in ensemble form.

VI. EXPERIMENTAL RESULTS

A. GP-TS inference strategies

A number of inference strategies for GP-TS were evaluated using the CSIR dataset. These include decoupled heteroscedastic GP-TS inference (DH-GP-TS), decoupled heteroscedastic GP-TS inference using sparse GP's (DH-SGP-TS), automatic differentiation variational inference under the fully Bayesian GP-TS model (ADVI-GP-TS) and automatic differentiation variational inference under the fully Bayesian GP-TS model using sparse GP's (ADVI-SGP-TS). Inception V3 bottleneck features were used for GP covariance function evaluations.

Table I shows the comparison prediction accuracy obtained using each of these approaches, when all available comparison outcomes were used for inference, and trained models used to predict comparison outcomes in the test set. The number of iterations used for inference are denoted by k , while M denotes the number of inducing image features used by the sparse Gaussian process. These features are selected by K -means clustering the image features in the training set. Prediction accuracy refers to the fraction of game outcomes

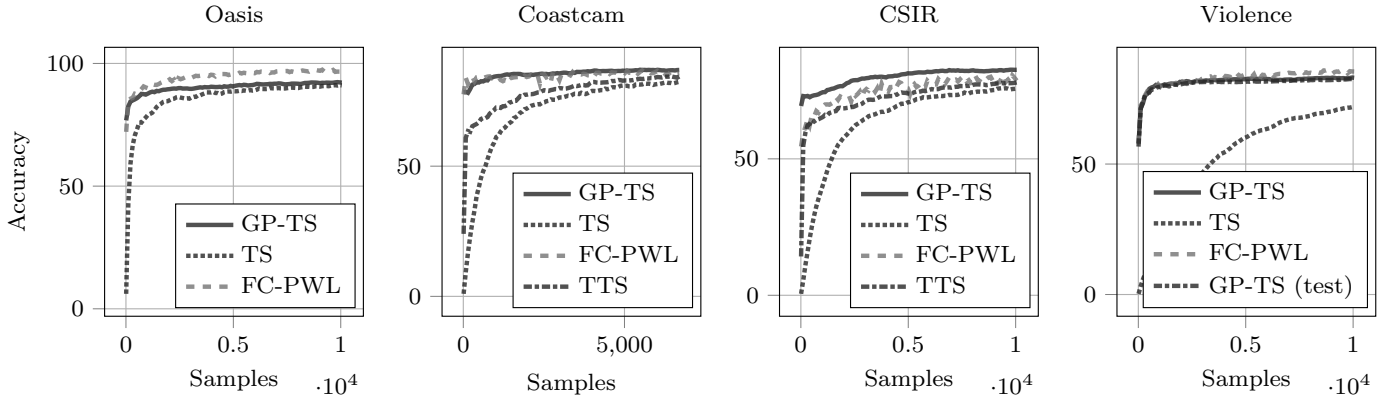


Fig. 3. Traces of the image comparison prediction accuracy as the number of samples used for model training is increased highlight the performance of GP-TS. Note that temporal TrueSkill (TTS) was only used on the video datasets, as this approach requires sequential data. As the perceived violence dataset is already divided into test and train sets, we report the game prediction accuracy using test sets, $\mathbf{G}_{\text{test}}^2$, extracted from both training, $\mathbf{G}_{\text{baseline}}$, and test sets, $\mathbf{G}_{\text{baseline_test}}$, and a model trained on an increasing number of pairwise labels extracted from the training set, $\mathbf{G}_{\text{train}}$.

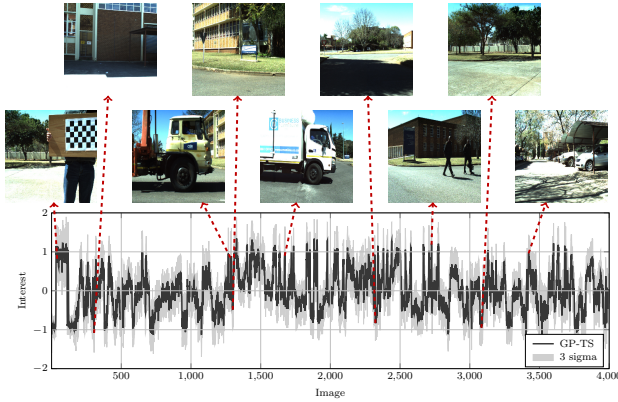


Fig. 4. Image samples with higher interest scores tend to contain vehicles or pedestrians (in line with the operator’s preference), while image samples with lower interest scores are generally empty road scenes or images of buildings.

that were correctly predicted by computing the posterior predictive probability of each image winning a comparison game outcome. This probability is thresholded, under the assumption that a game outcome is correct if the predicted probability in favour of the image winning the game is greater than 50 %.

Interestingly, decoupling the inference phases proved far more effective than performing inference under a fully Bayesian model, presumably because the inference task is simplified dramatically through this decoupling, as evidenced by the small number of expectation propagation iterations (k) required for inference in this case. The sparse GP approximation produces a moderate performance drop, but with substantial reduction in computational time. In light of these results, all experiments are conducted using DH-GP-TS for the remainder of this paper, which is termed GP-TS for brevity.

B. Interest prediction

Four interest detection algorithms were compared: A TrueSkill interest estimate (TS) [23], a temporally smoothed interest algorithm (TTS) [10], the proposed GP interest estimation approach, GP-TS, and a deep pairwise ranking

TABLE I
INFERENCE STRATEGY EFFICACY

	Parameters	Time (mm:ss)	Acc. (%)
DH-GP-TS	$k=5$	1:56	80.89
DH-SGP-TS	$k=5, M=100$	0:47	77.43
ADVI-GP-TS	$k=200$	45:18	74.79
ADVI-SGP-TS	$k=200, M=100$	1:24	73.56

approach, FC-PWL. Both GP-TS and FC-PWL use image features extracted using the Inception-V3 convolutional neural network, pre-trained for image classification on the ImageNet database [48]. The FC-PWL model uses 3 fully connected layers comprising 2 048, 1 024 and 1 neurons respectively, and was trained for 50 epochs using the Adam optimiser with parameters defined as in [29] and a batch size of 256. These parameters were chosen because they produced the most reliable results across all datasets.

Figure 3 shows traces of the image comparison prediction accuracy for each algorithm, on each of the first four test datasets. Here, an increasing number of comparisons sampled from training sets, $\mathbf{G}_{\text{train}}$, were used to predict game outcomes for the comparison pairs in \mathbf{G}_{test} , for each of the four datasets. Note that the results of the proposed approach are also shown for the test set of the violence dataset, $\mathbf{G}_{\text{test}}^2$, but with models still trained using subsets of the training set, $\mathbf{G}_{\text{train}}$. In the case of the non-probabilistic FC-PWL approach, game winners were predicted by selecting the image producing the largest logit predicted by the neural network pairs.

Figure 4 shows the posterior predictions for GP-TS when all 15 000 comparisons are used for interest estimation on the CSIR dataset, along with a selection of images corresponding to various interest levels. Images with higher interest scores contain objects of interest (pedestrians or vehicles), while images with lower image interest scores are more likely to be of empty road scenes.

It is clear that GP-TS outperforms the interest estimation of TTS and TS. Smoothing in image feature space requires

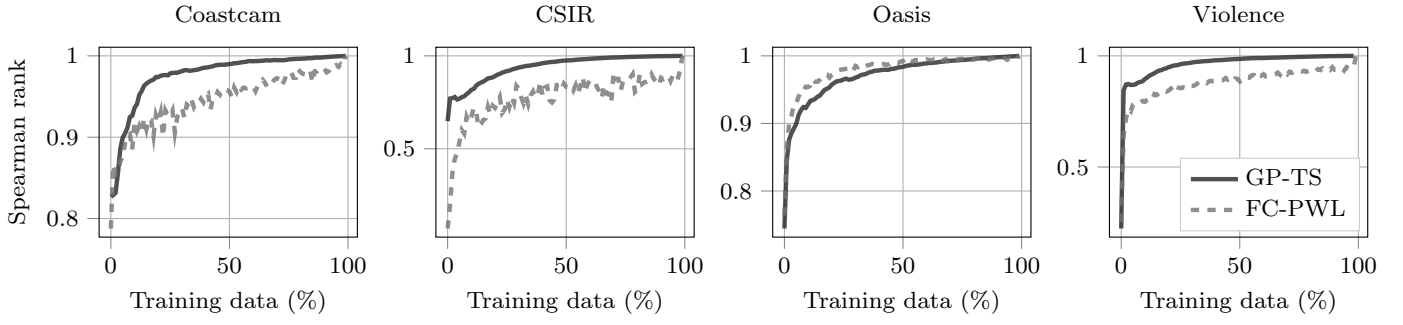


Fig. 5. Spearman rank correlations between final rankings obtained using all training data and those trained with limited labelling show that GP-TS tends to converge to the true rank faster than a FC-PWL, indicating that it is more sample efficient.

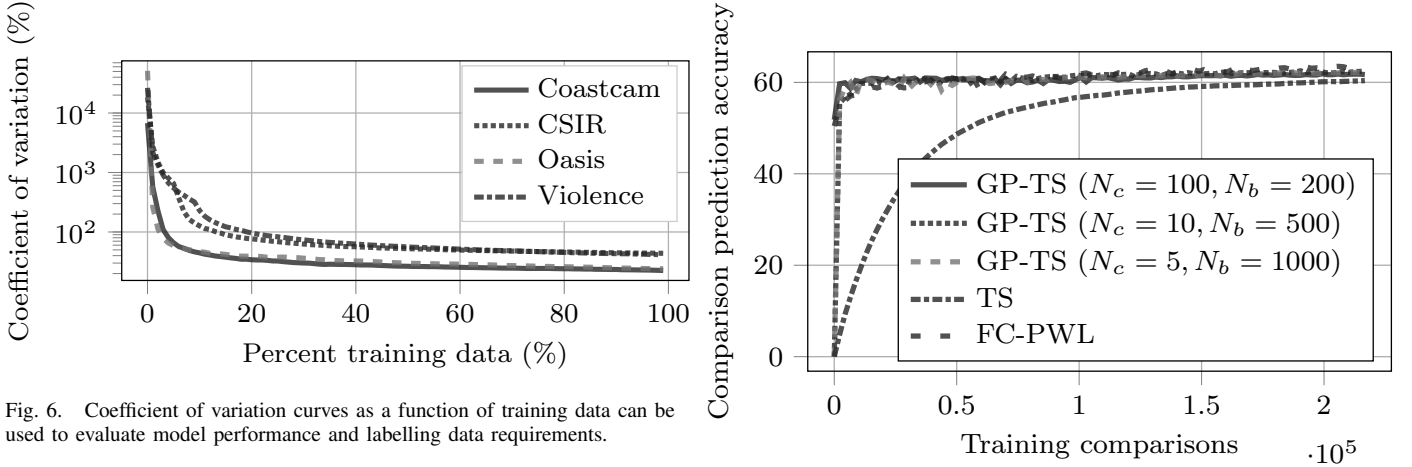


Fig. 6. Coefficient of variation curves as a function of training data can be used to evaluate model performance and labelling data requirements.

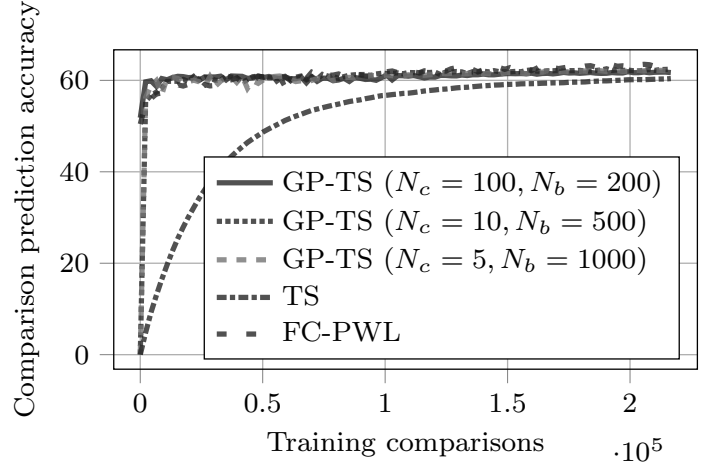


Fig. 7. Traces of the image comparison prediction accuracy as the number of samples used for model training is increased show that an ensemble of GP-TSs exhibits similar convergence results to those obtained using individual regressors.

significantly fewer training comparisons to outperform the baseline probabilistic interest prediction algorithms. TTS results are only provided for sequential image datasets, as this approach requires video or image sequences. FC-PWL performs similarly to GP-TS, outperforming the latter on the simpler OASIS dataset, but under-performing on the CSIR dataset. It should be noted that FC-PWL needed to be hand tuned to find parameters that worked across each dataset, relying on neural network designer skills and experience to do so. In contrast, the GP-TS approach requires no design expertise, as all parameters are inferred automatically.

More importantly, the GP-TS approach is more sample efficient, and produces better ranking estimates with limited labelling data. This is visible when the Spearman rank correlation is measured between the image interests inferred using only a portion of the training data, and those inferred using all available data (Figure 5). This is true for all but the Oasis dataset, which is simple enough to rank using relatively few image comparisons.

C. Uncertainty analysis

The combination of the Gaussian process with TrueSkill means that GP-TS is a probabilistic model and image interest predictions are paired with a variance measure. This measure captures the uncertainty in an interest prediction, but also uncertainty due to inconsistent labelling, which may occur

due to labelling error, or simply because images compared have similar interest values. These probabilistic estimates are particularly valuable, as they can be used to propose comparisons to present within an active labelling framework, or to select interesting content to show to users while taking into account the potential uncertainty therein. Figure 6 shows the average coefficients of variation (the average ratio of the predicted standard deviation to the absolute value of the predicted mean interest) as a function of the number of pairwise comparisons used for inference using each of the test datasets. As expected, the predictions become more certain (less volatile) with additional comparisons. Convergence to a stable estimate is obtained after relatively few comparisons. The accompanying video shows how uncertainty and interest changes during the training process.

The ability to estimate the uncertainty in inferred image interests is particularly valuable, as it can be used as a convergence measure to decide when enough comparisons have been captured during a dataset labelling process. Current state of the art methods such as FC-PWL, which only provide point-estimate predictions, require that a large test set be captured in order to test model accuracy and evaluate

algorithm performance so as to determine how much labelling data is required to train a reliable model. Further, there are no guarantees regarding the certainty in individual image interest predictions using these approaches and no existing mechanisms for determining when sufficient labelling has occurred.

D. Scaling to large datasets

As mentioned previously, Gaussian processes are often deemed unsuitable for large datasets as they are memory intensive. However, ensemble approaches can be used to remedy this. Figure 7 shows the results obtained when an ensemble of GP-TSs is used to predict the perceived safety of a street scene using training data sampled from the Place Pulse 2.0 dataset [17]. Experimental results provided follow the same procedures as before, but here N_e Gaussian processes were trained to predict TrueSkill interests using batches of N_b images sampled from the dataset. It is clear that the ensemble exhibits similar convergence results to those seen previously, and is relatively robust to parameter choices.

Table II shows the percentage area under the curve (relative to the maximum possible area) for each method on the various datasets of interest, and provides ablation results when the pre-trained features used as inputs to GP-TS are varied. Here, Inception-V3 [48], Resnet50 [21], VGG16 [45] and Histogram of Oriented Gradient (HoG) [13] features are used for testing.

GP-TS and FC-PWL perform similarly with less training data, but, as expected, FC-PWL performance improves when substantially more data is available. Ablation results show that pre-trained convolutional network and HoG features used by GP-TS produce generally similar results, although HoG performance drops for more challenging datasets. Due to computational limitations, experiments on Place Pulse 2.0 were only conducted using Inception-V3 features.

GP-TS can be trained in a few minutes on smaller datasets comprising only a few thousand images (12 Core-i7 CPU, 16 GB RAM), but slows significantly on extremely large datasets due to the GP's $\mathcal{O}(n^3)$ memory requirements. Ensembles and batched variational inference strategies remedy this to an extent, but deep learning approaches like FC-PWL, which can be trained more efficiently, are better suited to extremely large datasets, where sample efficiency is not required.

E. Saliency

An occlusion-based sensitivity analysis technique [59] was applied to the trained models in order to investigate whether GP-TS is actually identifying image content of interest, or simply fitting to the data. Here, a blanking window is slid over the image, and the resultant change in predicted image interest measured at these blanked locations. Figure 8 shows the 5 most interesting images in four test datasets, along with sensitivity maps.

It is clear that the model has learned to associate brain ventricles with interest in the Oasis dataset, while fire is highlighted in the violence dataset. In contrast, people and cars seem to be considered interesting in the CSIR set, while

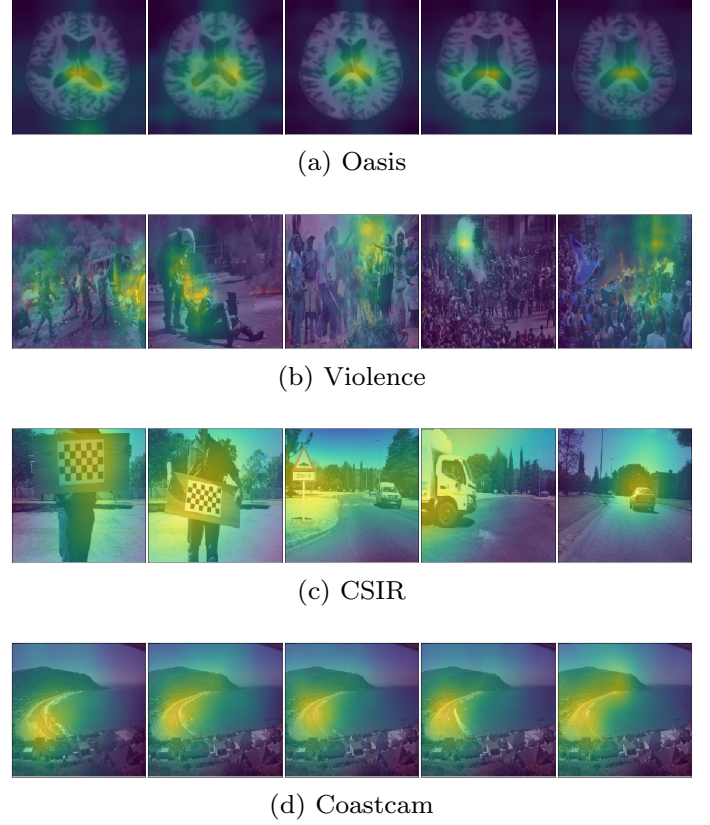


Fig. 8. Saliency maps show that the interest prediction model has identified content of interest to the end user.

the coastline is associated with image interest for the Coastcam dataset.

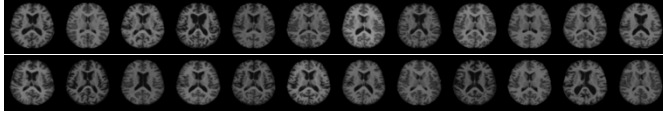
F. Storyboarding

Figure 9 shows 24-image storyboard summaries of the OASIS data set produced using GP-TS, MemNet and HAC. GP-TS storyboards were produced using both 100% and 20% of the available training data so as to highlight the rapid convergence to good interest estimates obtained using this approach. The GP-TS storyboard contains images likely to be of interest to an end user. In contrast, many commonly used storyboarding schemes lack the user-driven context of the proposed interest-based approach. Hierarchical agglomerative clustering produces a diverse set of images showing the range of healthy and unhealthy brains in the dataset, as the clustering rewards image dissimilarity, but many of the images produced are not of interest to an end-user. MemNet identifies a diverse range of images, but these fail to align with user preferences, while GP-TS has identified brains with enlarged ventricles as interesting.

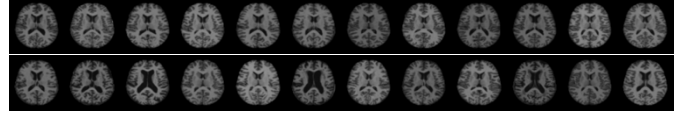
This is particularly noticeable if we consider the Coastcam storyboards shown in Figure 10. Here, HAC tends to show a diverse set of coastal conditions, which are certainly interesting to a general audience. MemNet restricts images in the storyboard to daylight images, but these storyboard images contrast significantly with the domain-specific interests

TABLE II
% AREA UNDER CURVE (PREDICTION ACCURACY VS TRAINING DATA)

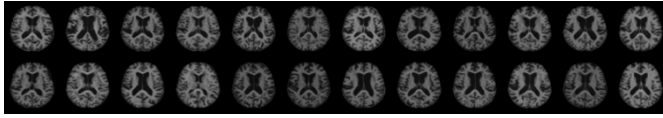
	OASIS	Violence	CSIR	Coastcam	Place Pulse 2.0
GP-TS					
HoG	89.29	69.12	72.57	84.87	-
Inception-V3	90.27	80.43	79.86	85.43	60.84
ResNet50	90.85	82.44	78.81	85.85	-
VGG16	90.69	81.32	78.48	85.35	-
TS	85.60	52.66	63.84	70.86	51.25
TTS	-	-	72.22	78.08	-
FC-PWL	94.59	82.83	75.20	84.87	61.29



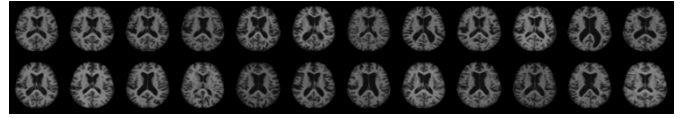
(a) Clustering



(b) MemNet



(c) GP-TS (20%)

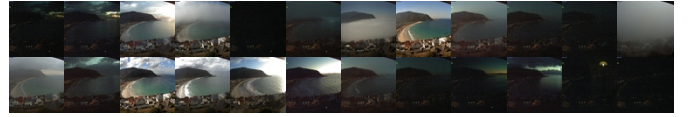


(d) GP-TS (100%)

Fig. 9. OASIS dataset storyboards created using HAC, MemNet, and GP-TS show the range of brain scans in the dataset. Here, interesting images are those with reduced brain volume, typically indicated by enlarged central ventricles filled with fluid (coloured black).



(a) MemNet



(b) Clustering



(c) GP-TS (20 %)



(d) GP-TS (100 %)

Fig. 10. The figure shows Coastcam dataset storyboards created using HAC, MemNet, and GP-TS. GP-TS storyboarding selects images with clearly differentiable wet and dry shoreline areas, and where the waves are in a backwash phase, in line with user preferences.



(a) Clustering



(b) MemNet



(c) GP-TS (20 %)



(d) GP-TS (100 %)

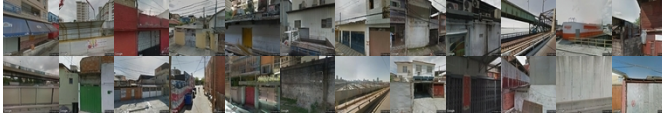
Fig. 11. Perceived violence dataset storyboards created using HAC, MemNet, and GP-TS highlight the differences between memorability and domain specific interest in violence.



(a) Random sampling



(b) MemNet



(c) GP-TS (20 %)



(d) GP-TS (100 %)

Fig. 12. Place Pulse 2.0 dataset storyboards created using random sampling, MemNet, and GP-TS highlight the differences between memorability and domain specific interest in street scene safety.

TABLE III
NUMBER OF INTERESTING IMAGES PER STORYBOARD

	MemNet	HAC	GP-TS 20 %	GP-TS 100 %
OASIS	5	12	22	22
Violence	0	1	19	24
CSIR	17	15	23	24
Coastcam	9	1	24	24
Place Pulse	5	-	24	24

of coastal scientists seeking to study soil erosion, as they fail to flag images with clearly distinguishable wet and dry sand regions.

The differences in storyboarding are even more stark when the Violence dataset is summarised using GP-TS, HAC and MemNet (Figure 11). HAC shows the broad range of images present in the dataset, MemNet seems to show a preference for signage, while GP-TS flags images with fire and fallen people as interesting. Similar results are visible when a storyboard of the Place Pulse 2.0 dataset is produced (Figure 12). HAC is not used here, due to memory limitations.

While it is clear that general purpose image summarising tools have their place, the storyboarding task above serves as an important reminder that in many instances, domain specific problems need to be solved. Here, image interest is often both task and problem dependent. This is highlighted by the simple count of interesting images present per storyboard provided in Table III.

VII. MEMORABILITY AND INTEREST

The relationship between image memorability and image interest warrants further investigation. Table IV shows the Pearson correlation coefficients ρ measured between memorability scores obtained using MemNet [26] and the domain-specific image interest predictions produced using GP-TS for each of the five test datasets, using all available pairwise comparisons for inference.

Interestingly, memorability correlates the most with the interest scores obtained for the Coastcam database. This is potentially due to the fact that the coastal images of interest are typically captured in bright sunlight and are generally aesthetically pleasing, while there are a large number of

TABLE IV
MEMORABILITY VS INTEREST

	OASIS	Violence	CSIR
ρ	-0.2	-0.47	0.04
	Coastcam	Place Pulse 2.0	
ρ	0.7	-0.32	

dark images captured at night. There is a moderate negative correlation between image memorability and both the interests inferred from perceived violence measures and the street scene safety assessments in the Place Pulse 2.0 dataset. Similar results are obtained when measuring the correlation between memorability predictions and perceived violence scores directly ($\rho = -0.42$). This contrasts somewhat with the findings in [26], which showed that there was little to no correlation between the aesthetic score of an image and its memorability, and that images that evoke anger and fear tend to be more memorable.

It should be noted that the memorability predictions are made using a network that was trained using 60 000 images obtained from general image collections, and comprises both object-centric and scene-centric images, together with images of objects taken from unconventional angles, but was used in an entirely unsupervised manner here. As a result, it is possible that the memorability predictions are failing on the datasets investigated here.

VIII. CONCLUSIONS

This paper has introduced a probabilistic pairwise ranking approach, GP-TS. Standard probabilistic ranking algorithms using pairwise comparisons like these typically require a large number of comparisons, but this work has shown that pairing these with a Gaussian process smoother dramatically reduces this number, by making use of similarities between image features extracted using a pre-trained convolutional neural network.

A primary benefit of GP-TS is that it produces a probability distribution over image interests. The uncertainty in these interest estimates can be used to select images to a present to a user for labelling, as part of an active learning process, but also to determine if sufficient data labelling has taken place.

This work has also argued that image interest is often domain and task specific. A great deal of work has investigated general forms of image interest or memorability measures, but it is important to note that these measures are not always suitable for end-users. While there is indeed great value in collecting large scale datasets suitable for training general image interest and memorability scores, and this is extremely important for algorithm evaluation, practical deployments of efficient computer vision systems often require task specific algorithms that can be rapidly trained on small scale datasets.

- [1] Dynamo guidelines for academic requesters on Amazon Mechanical Turk. Online, August 2016. URL http://wiki.wearedynamo.org/index.php/Guidelines_for_Academic_Requesters.
- [2] MediaEval 2018. Online, March 2018. URL <http://www.multimediaeval.org/mediaeval2018/>.
- [3] Omid Aghazadeh, Josephine Sullivan, and Stefan Carlsson. Novelty detection from an ego-centric perspective. In *Computer Vision and Pattern Recognition (CVPR), 2011 IEEE Conference on*, pages 3297–3304. IEEE, 2011.
- [4] Olfa Ben-Ahmed, Jonas Wacker, Alessandro Gaballo, and Benoit Huet. EURECOM MediaEval 2017: Media genre inference for predicting media interestingness. In *Working Notes Proceedings of the MediaEval 2017 Workshop*. CEUR Workshop Proceedings, 2017.
- [5] Dima Damen, Osian Haines, Teesid Leelasawassuk, Andrew Calway, and Walterio Mayol-Cuevas. Multi-user egocentric online system for unsupervised assistance on object usage. In *Computer Vision-ECCV 2014 Workshops*, pages 481–492. Springer, 2014.
- [6] Claire-Hélène Demarty, Mats Sjöberg, Bogdan Ionescu, Thanh-Toan Do, Michael Gygli, and Ngoc Q.K. Duong. MediaEval 2017 predicting media interestingness task. In *Working Notes Proceedings of the MediaEval 2017 Workshop*. CEUR Workshop Proceedings, 2017.
- [7] Christopher P Dieh, John B Hampshire, et al. Real-time object classification and novelty detection for collaborative video surveillance. In *Neural Networks, 2002. IJCNN'02. Proceedings of the 2002 International Joint Conference on*, volume 3, pages 2620–2625. IEEE, 2002.
- [8] Abhimanyu Dubey, Nikhil Naik, Devi Parikh, Ramesh

- Raskar, and César A Hidalgo. Deep learning the city: Quantifying urban perception at a global scale. In *European Conference on Computer Vision*, pages 196–212. Springer, 2016.
- [18] Arpad E Elo. *The rating of chessplayers, past and present*. Arco Pub., 1978.
- [19] Onur G. Guleryuz and Viresh Ratnakar. Multiresolutional descriptions of digital video in terms of relevance. In *Proc. IASTED Int’l Conf. on Signal and Image Proc. (SIP2001)*, August 2001.
- [20] Severin Hacker and Luis von Ahn. Matchin: Eliciting user preferences with an online game. In *Proceedings of the SIGCHI Conference on Human Factors in Computing Systems*, CHI ’09, pages 1207–1216, New York, NY, USA, 2009. ACM.
- [21] Kaiming He, Xiangyu Zhang, Shaoqing Ren, and Jian Sun. Deep residual learning for image recognition. In *Proceedings of the IEEE conference on computer vision and pattern recognition*, pages 770–778, 2016.
- [22] Ralf Herbrich, Neil D Lawrence, and Matthias Seeger. Fast sparse Gaussian process methods: The informative vector machine. In *Advances in neural information processing systems*, pages 625–632, 2003.
- [23] Ralf Herbrich, Tom Minka, and Thore Graepel. Trueskill™: A Bayesian skill rating system. In *Advances in neural information processing systems*, pages 569–576, 2006.
- [24] Jeroen HM Janssens. Ranking images on semantic attributes using human computation. In *NIPS workshop on computational social science and the Wisdom of crowds*, 2010.
- [25] Thorsten Joachims. Optimizing search engines using clickthrough data. In *Proceedings of the eighth ACM SIGKDD international conference on Knowledge discovery and data mining*, pages 133–142. ACM, 2002.
- [26] Aditya Khosla, Akhil S. Raju, Antonio Torralba, and Aude Oliva. Understanding and predicting image memorability at a large scale. In *International Conference on Computer Vision (ICCV)*, 2015.
- [27] M Hadi Kiapour, Kota Yamaguchi, Alexander C Berg, and Tamara L Berg. Hipster wars: Discovering elements of fashion styles. In *European conference on computer vision*, pages 472–488. Springer, 2014.
- [28] H. Kim, T. Mei, H. Byun, and T. Yao. Exploiting web images for video highlight detection with triplet deep ranking. *IEEE Transactions on Multimedia*, pages 1–1, 2018. ISSN 1520-9210. doi: 10.1109/TMM.2018.2806224.
- [29] Diederik P Kingma and Jimmy Ba. Adam: A method for stochastic optimization. *arXiv preprint arXiv:1412.6980*, 2014.
- [30] Alp Kucukelbir, Dustin Tran, Rajesh Ranganath, Andrew Gelman, and David M Blei. Automatic differentiation variational inference. *The Journal of Machine Learning Research*, 18(1):430–474, 2017.
- [31] Quoc V Le, Alex J Smola, and Stéphane Canu. Heteroscedastic gaussian process regression. In *Proceedings of the 22nd international conference on Machine learning*, pages 489–496. ACM, 2005.
- [32] Y. Liu and T. Mei. Optimizing visual search reranking via pairwise learning. *IEEE Transactions on Multimedia*, 13(2):280–291, April 2011. ISSN 1520-9210. doi: 10.1109/TMM.2010.2103931.
- [33] L. Ma, L. Xu, Y. Zhang, Y. Yan, and K. N. Ngan. No-reference retargeted image quality assessment based on pairwise rank learning. *IEEE Transactions on Multimedia*, 18(11):2228–2237, Nov 2016. ISSN 1520-9210. doi: 10.1109/TMM.2016.2614187.
- [34] P.J. Macer and P.J. Thomas. Video storyboards: summarising video sequences for indexing and searching of video databases. In *Intelligent Image Databases, IEE Colloquium on*, pages 2/1–2/5, May 1996. doi: 10.1049/ic:19960740.
- [35] Daniel S Marcus, Tracy H Wang, Jamie Parker, John G Csernansky, John C Morris, and Randy L Buckner. Open access series of imaging studies (OASIS): cross-sectional MRI data in young, middle aged, nondemented, and demented older adults. *Journal of cognitive neuroscience*, 19(9):1498–1507, 2007.
- [36] Thomas P Minka. *A family of algorithms for approximate Bayesian inference*. PhD thesis, Massachusetts Institute of Technology, 2001.
- [37] Partha Pratim Mohanta, Sanjoy Kumar Saha, and Bhabatosh Chanda. A novel technique for size constrained video storyboard generation using statistical run test and spanning tree. *International Journal of Image and Graphics*, 13(01):1350001, 2013.
- [38] N. Naik, J. Philipoom, R. Raskar, and C. Hidalgo. Streetscore – predicting the perceived safety of one million streetscapes. In *2014 IEEE Conference on Computer Vision and Pattern Recognition Workshops*, pages 793–799, June 2014.
- [39] Chong-Wah Ngo, Yu-Fei Ma, and Hong-Jiang Zhang. Video summarization and scene detection by graph modeling. *Circuits and Systems for Video Technology, IEEE Transactions on*, 15(2):296–305, Feb 2005. ISSN 1051-8215. doi: 10.1109/TCSVT.2004.841694.
- [40] CE Rasmussen and CKI Williams. Gaussian processes for machine learning, 2006.
- [41] Herbert E Rauch, CT Striebel, and F Tung. Maximum likelihood estimates of linear dynamic systems. *AIAA journal*, 3(8):1445–1450, 1965.
- [42] John Salvatier, Thomas V Wiecki, and Christopher Fonnesbeck. Probabilistic programming in python using pymc3. *PeerJ Computer Science*, 2:e55, 2016.
- [43] Andreza Sartori. Affective analysis of abstract paintings using statistical analysis and art theory. In *Proceedings of the 16th International Conference on Multimodal Interaction*, pages 384–388. ACM, 2014.
- [44] Yuesong Shen, Claire-Hélène Demarty, and Ngoc QK Duong. Technicolor MediaEval 2016 Predicting Media Interestingness Task. In *MediaEval*, 2016.

- [45] Karen Simonyan and Andrew Zisserman. Very deep convolutional networks for large-scale image recognition. *arXiv preprint arXiv:1409.1556*, 2014.
- [46] Savitha Srinivasan, Duke Ponceleon, Arnon Amir, and Dragutin Petkovic. “What is in that video anyway?”: in search of better browsing. In *Multimedia Computing and Systems, 1999. IEEE International Conference on*, volume 1, pages 388–393. IEEE, 1999.
- [47] W. T. Sun, T. H. Chao, Y. H. Kuo, and W. H. Hsu. Photo filter recommendation by category-aware aesthetic learning. *IEEE Transactions on Multimedia*, 19(8):1870–1880, Aug 2017. ISSN 1520-9210. doi: 10.1109/TMM.2017.2688929.
- [48] Christian Szegedy, Wei Liu, Yangqing Jia, Pierre Sermanet, Scott Reed, Dragomir Anguelov, Dumitru Erhan, Vincent Vanhoucke, and Andrew Rabinovich. Going deeper with convolutions. In *Proceedings of the IEEE Conference on Computer Vision and Pattern Recognition*, pages 1–9, 2015.
- [49] X. Tian, L. Yang, J. Wang, X. Wu, and X. S. Hua. Bayesian visual reranking. *IEEE Transactions on Multimedia*, 13(4):639–652, Aug 2011. ISSN 1520-9210. doi: 10.1109/TMM.2011.2111363.
- [50] Volker Tresp. A Bayesian committee machine. *Neural computation*, 12(11):2719–2741, 2000.
- [51] Patrizia Varini, Giuseppe Serra, and Rita Cucchiara. Personalized egocentric video summarization for cultural experience. In *Proceedings of the 5th ACM on International Conference on Multimedia Retrieval*, pages 539–542. ACM, 2015.
- [52] V. Vonikakis, R. Subramanian, J. Arnfred, and S. Winkler. A probabilistic approach to people-centric photo selection and sequencing. *IEEE Transactions on Multimedia*, 19(11):2609–2624, Nov 2017. ISSN 1520-9210. doi: 10.1109/TMM.2017.2699859.
- [53] Shuai Wang, Shizhe Chen, Jinming Zhao, Wenxuan Wang, and Qin Jin. Ruc at mediaeval 2017: Predicting media interestingness task. In *Working Notes Proceedings of the MediaEval 2017 Workshop*. CEUR Workshop Proceedings, 2017.
- [54] Joe H Ward Jr. Hierarchical grouping to optimize an objective function. *Journal of the American statistical association*, 58(301):236–244, 1963.
- [55] Chung-Lin Wen et al. Event-centric twitter photo summarization. Master’s thesis, Massachusetts Institute of Technology, 2014.
- [56] Heiko Wolf and Da Deng. How interesting is this? Finding interest hotspots and ranking images using an MPEG-7 visual attention model. *Annual Colloquium of Spatial Research Centre, (SIRC05)*, 2005.
- [57] Donghyeon Won, Zachary C Steinert-Threlkeld, and Jungseock Joo. Protest activity detection and perceived violence estimation from social media images. In *Proceedings of the 2017 ACM on Multimedia Conference*, pages 786–794. ACM, 2017.
- [58] Bo Xiong and Kristen Grauman. Detecting snap points in egocentric video with a web photo prior. In *Computer Vision–ECCV 2014*, pages 282–298. Springer, 2014.
- [59] Matthew D Zeiler and Rob Fergus. Visualizing and understanding convolutional networks. In *European conference on computer vision*, pages 818–833. Springer, 2014.
- [60] Jun-Yan Zhu, Aseem Agarwala, Alexei A Efros, Eli Shechtman, and Jue Wang. Mirror mirror: Crowdsourcing better portraits. *ACM Transactions on Graphics (TOG)*, 33(6):234, 2014.